

# Characterization by AERONET Sun Photometer of Aerosol Events with High Aerosol Optical Depth and Ångström Exponent over Sofia, Bulgaria

---

Tsvetina Evgenieva, Ljuan Gurdev, Eleonora Toncheva, Tanja Dreischuh

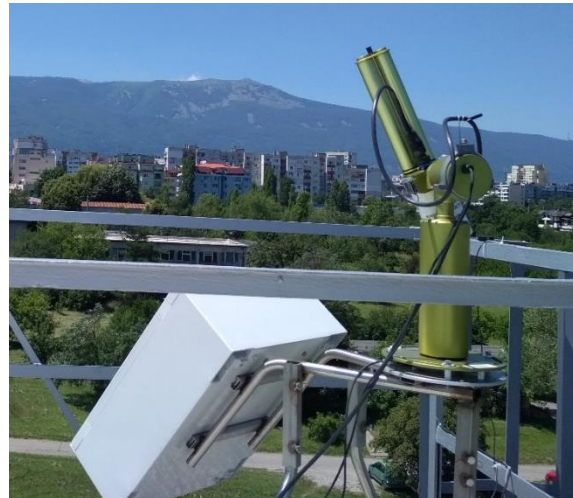
Institute of Electronics, Bulgarian Academy of Sciences,  
72 Tsarigradsko Chaussee Blvd., 1784 Sofia, Bulgaria  
e-mail: tsevgenieva@ie.bas.bg

# Sofia Site at the Institute of Electronics - BAS

- ❖ **European Aerosol Research Lidar Network (EARLINET)**
- ❖ **Aerosol, Clouds and Trace Gases Research Infrastructure (ACTRIS)** - a regular LIDAR monitoring is performed of the aerosol stratification over Sofia, Bulgaria
- ❖ **Aerosol RObotic NETwork (AERONET)** – a regular Cimel CE318-TS9 sun/sky/lunar photometer measurements are performed since 5 May 2020

**Map of Sofia Valley**

**Cimel CE318-TS9 sun/sky/lunar photometer**



- ❑ 9 channels with central wavelengths at  $\lambda = 340, 380, 440, 500, 675, 870, 937, 1020, 1640$  nm
- ❑ Field of view -  $1.3^\circ$
- ❑ Direct sun irradiance - every 3 - 5 min
- ❑ Sky radiances – in general every hour at several wavelengths

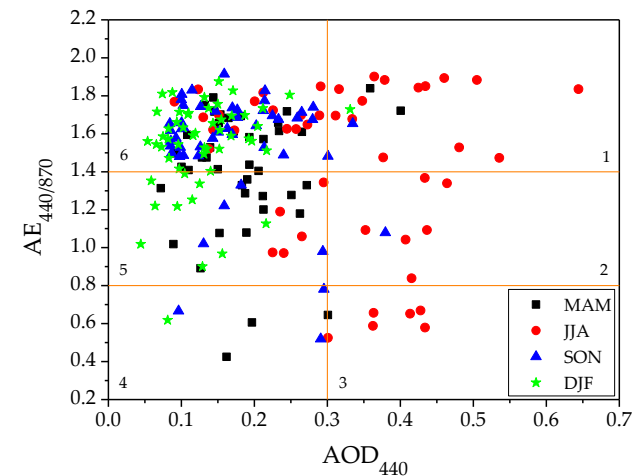
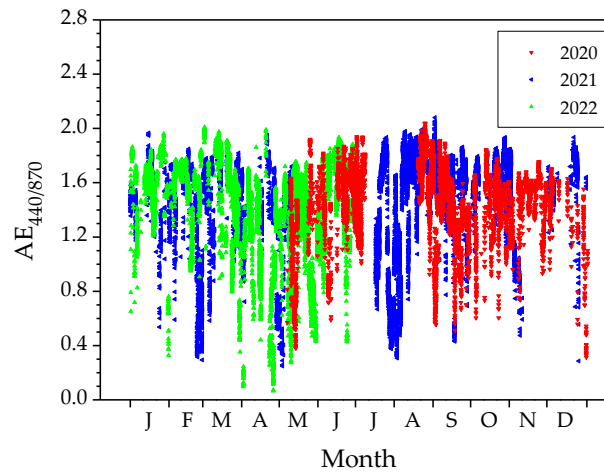
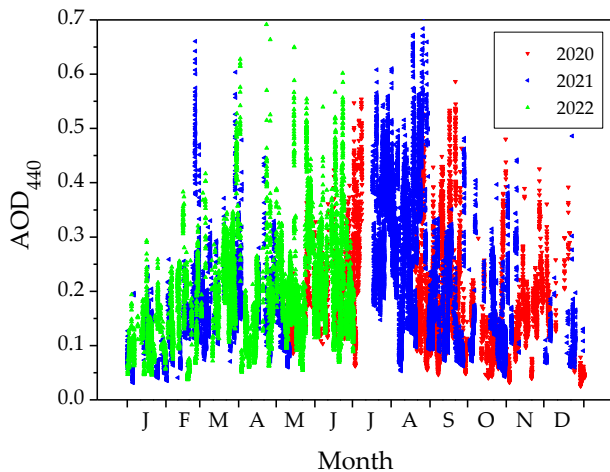
# Aim

To analyze the results of two-year passive optical remote sensing of the atmospheric aerosol field over Sofia, Bulgaria, and characterize mainly the aerosol situations with a strongly prevailing fine particle fraction of a relatively high turbidity during summer, autumn and winter

Special attention is given to cases of fresh biomass-burning (BB) aerosols with high aerosol optical depth at  $\lambda = 440$  nm ( $AOD_{440} > 0.3$ ) and Ångström exponent ( $AE_{440/870} > 1.6 - 1.7$ ), high sphericity factor ( $SF > 0.9$ ) and low depolarization ratio ( $DR \sim 0.002$ )

Variations of  $AOD_{440}$  and  $AE_{440/870}$  obtained in 2020, 2021 and 2022

Scatter plot of  $AOD_{440}$  vs.  $AE_{440/870}$  for the period 01.03.2021 - 28.02.2022



# Characterizing the Aerosol Types

## ➤ Main aerosol characteristics employed

AERONET daily mean values of the aerosol optical depths  $AOD_{440}$ ,  $AOD_{500}$ ,  $AOD_{f500}$ , and  $AOD_{c500}$ , and of the Ångström exponent  $AE_{440/870}$ , and range of the retrieved values of the particle sphericity factor (SF) and linear depolarization ratio (DR) for the days of concern in the work.

Date	$AOD_{440}$	$AOD_{500}$	$AOD_{f500}$	$AOD_{c500}$	$AE_{440/870}$	SF	DR
<b>25.11.2020</b>	0.35±0.03	0.31±0.03	0.29±0.02	0.02±0.002	1.11±0.06	0.96–0.99	0.004–0.007
<b>24.08.2021</b>	0.50±0.03	0.42±0.03	0.40±0.03	0.01±0.001	1.88±0.02	0.97–0.99	0.002–0.003
<b>28.08.2021</b>	0.54±0.05	0.46±0.04	0.43±0.04	0.03±0.007	1.47±0.07	0.34–0.99	0.002–0.090
<b>14.02.2022</b>	0.33±0.02	0.27±0.01	0.25±0.02	0.02±0.001	1.72±0.03	0.99	0.002–0.003

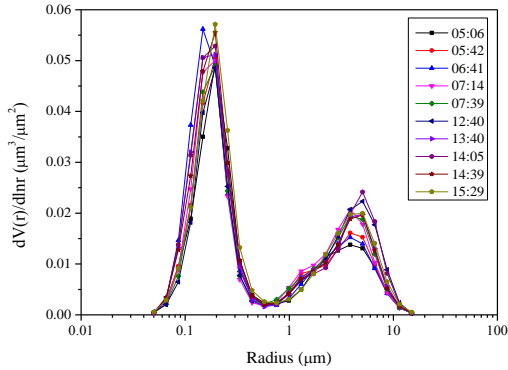
Range of the retrieved particle effective and volume median radii: total -  $R_{effT}$  and  $R_{mT}$ , of the fine fraction -  $R_{effF}$  and  $R_{mF}$ , and of the coarse fraction -  $R_{effC}$  and  $R_{mC}$ , for the days of concern in the work.

Date	$R_{effT}$ (μm)	$R_{mT}$	$R_{effF}$ (μm)	$R_{mF}$	$R_{effC}$ (μm)	$R_{mC}$
<b>25.11.2020</b>	0.25–0.31	0.45–0.51	0.20–0.24	0.25–0.29	2.76–2.85	3.36–3.50
<b>24.08.2021</b>	0.21–0.28	0.41–0.67	0.15–0.17	0.16–0.19	2.46–3.00	3.07–3.60
<b>28.08.2021</b>	0.33–0.36	0.59–0.62	0.21–0.25	0.23–0.28	2.04–2.34	2.42–2.67
<b>14.02.2022</b>	0.28–0.30	0.52–0.58	0.20	0.23	2.88–2.97	3.37–3.43

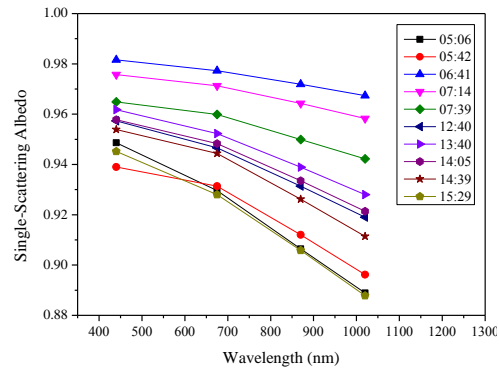
## ➤ Additional information – NOAA’s HYSPLIT air mass back trajectory model, BSC DREAM8b v2.0 desert dust forecasting model, NASA’s Fire Information for Resource Management System (FIRMS) and meteorological data

# Results

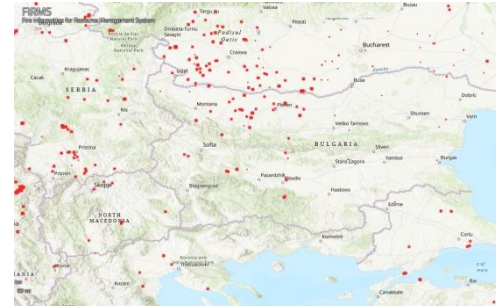
## AERONET Volume Size Distribution (VSD)



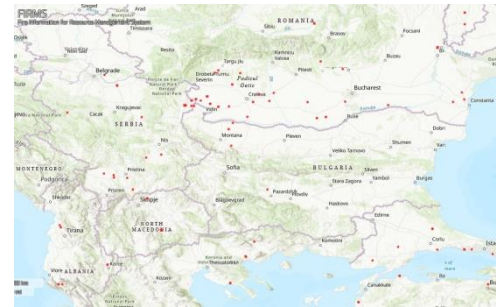
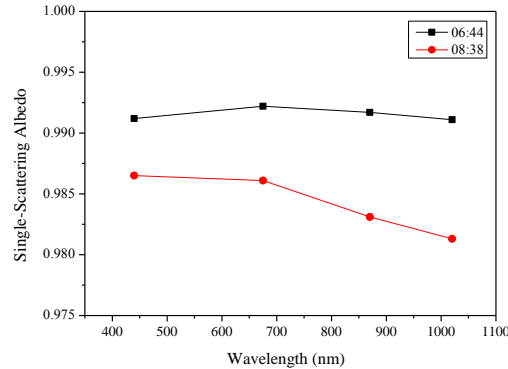
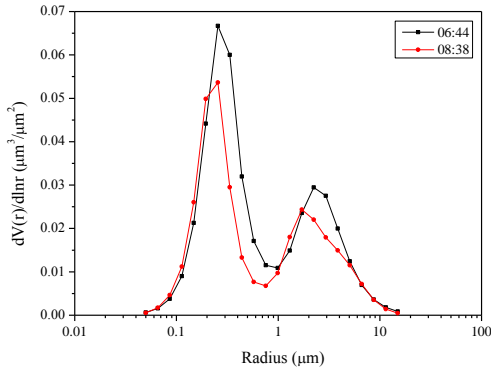
## AERONET Single-Scattering Albedo (SSA)



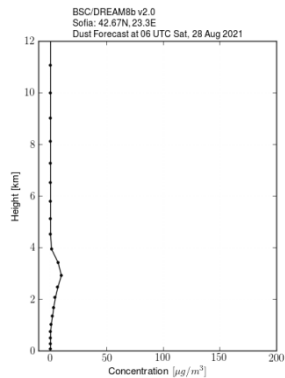
## NASA's FIRMS



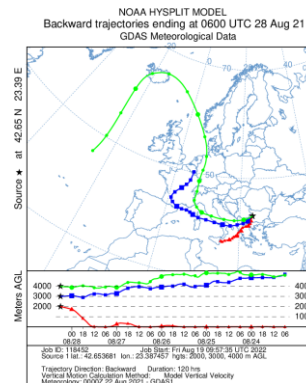
24.08.2021



28.08.2021



**BSC-DREAM8b**  
28.08.2021



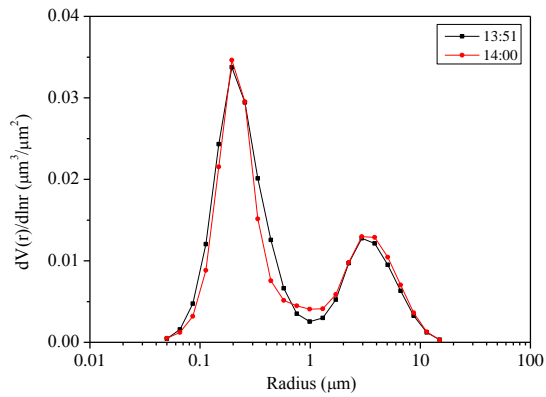
**NOAA's HYSPLIT**  
28.08.2021



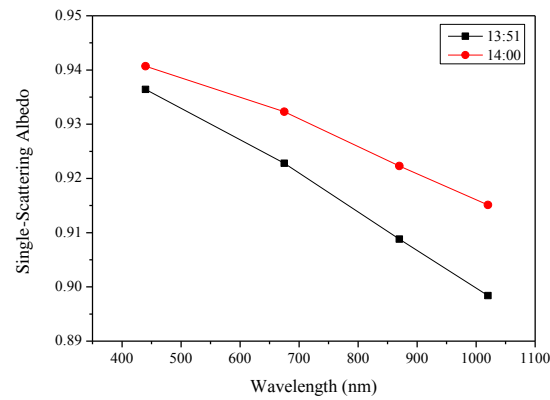
# Results

## AERONET VSD

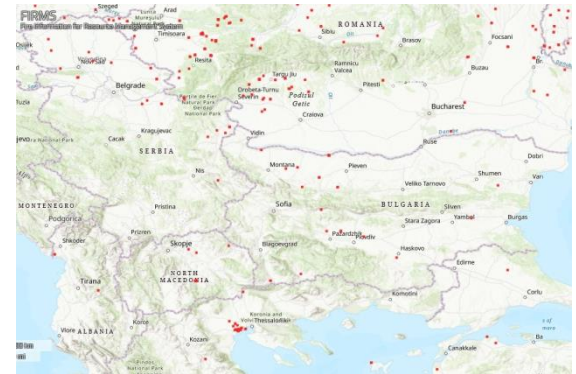
14.02.2022



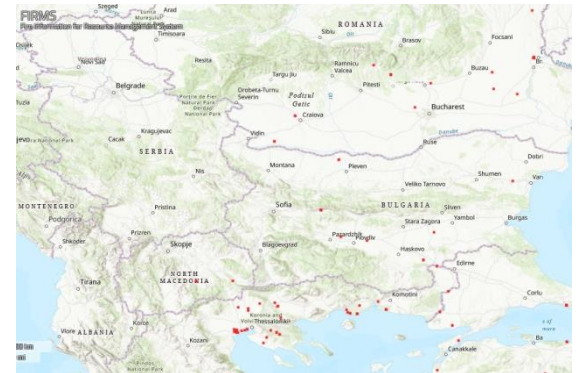
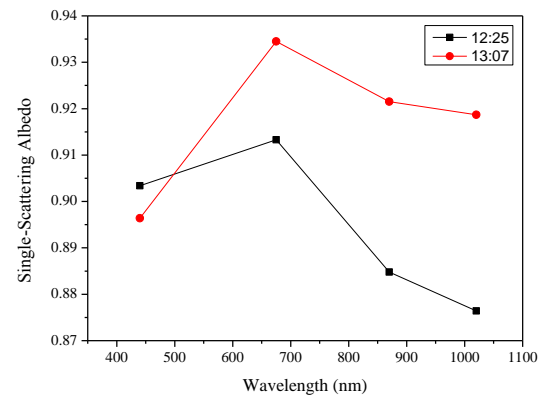
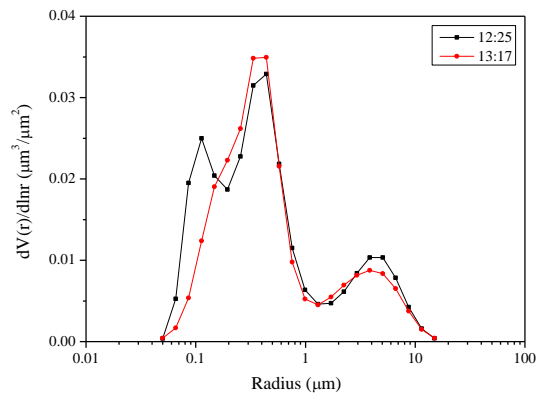
## AERONET SSA



## NASA's FIRMS



25.11.2020



# Conclusion

- Different high- $\text{AOD}_{440}$  and high- $\text{AE}_{440/870}$  biomass-burning aerosol situations take place mainly in summer and early autumn, because of intensive wildfire activity, but they may occur sometimes in winter and late autumn as consequence of domestic heating with wood and coal
- The BB fresh-aerosol optical and microphysical characteristics of the autumn-to-winter season are similar to that of the summer-to-autumn one
- The aged BB smoke fine particles have usually undergone an increase of the particle size leading to lowering  $\text{AE}_{440/870}$  values and modifying the dependence  $\text{SSA}$  vs.  $\lambda$

# Acknowledgments

This research was funded by the Ministry of Education and Science of Bulgaria (support for ACTRIS BG, part of the Bulgarian National Roadmap for Research Infrastructure), by the European Commission under the Horizon 2020 – Research and Innovation Framework Program, Grant Agreement No. 871115 (ACTRIS IMP), and by the Bulgarian National Science Fund (Grant No. KP-06-N28/10/2018). The authors acknowledge AERONET-Europe for providing calibration service. AERONET-Europe is part of ACTRIS-IMP project that received funding from the European Union (H2020-INFRADEV-2018-2020) under Grant Agreement No 871115. The NOAA Air Resources Laboratory is acknowledged for the provision of the HYSPLIT transport and dispersion model and the READY website used in this publication. The authors also acknowledge the images from the BSC-DREAM8b model operated by the Barcelona Supercomputing Center (<http://www.bsc.es/ess/bsc-dust-daily-forecast/>) and from NASA's Fire Information for Resource Management System (FIRMS) (<https://earthdata.nasa.gov/firms>), part of NASA's Earth Observing System Data and Information System (EOSDIS)